

Vortex lattices in Bose-Einstein condensates with Dipolar Interactions Beyond the Weak Interaction Limit

S. Komineas^{1,2} and N. R. Cooper¹

¹*Theory of Condensed Matter Group, Cavendish Laboratory,
J.J. Thomson Avenue, Cambridge CB3 0HE, United Kingdom*

²*Max-Planck Institute for the Physics of Complex Systems, Nöthnitzer Str. 38, 01187, Dresden, Germany.*

(Dated: November 17, 2006)

We study the ground states of rotating atomic Bose-Einstein condensates with dipolar interactions. We present the results of numerical studies on a periodic geometry which show vortex lattice ground states of various symmetries: triangular and square vortex lattices, “stripe crystal” and “bubble crystal”. We present the phase diagram (for systems with a large number of vortices) as a function of the ratio of dipolar to contact interactions and of the chemical potential. We discuss the experimental requirements for observing transitions between vortex lattice groundstates via dipolar interactions. We finally investigate the stability of mean-field supersolid phases of a quasi-2D *non*-rotating Bose gas with dipolar interactions.

PACS numbers:

I. INTRODUCTION

One of the most dramatic manifestations of the collective quantum behaviour of a Bose-Einstein condensate is its unusual response to rotation. The formation of quantised vortex lines, around which the phase of the condensate wavefunction changes by 2π , is a direct consequence of the existence of a collective phase-coherent quantum state. The further ordering of quantised vortices at low temperatures into regular vortex lattices is a signature not just of Bose-Einstein condensation but of the presence of non-zero (repulsive) interactions between the constituent particles.

Techniques for rotating condensates in ultra-cold atomic gases are now well established, and have led to very beautiful demonstrations of the physics of quantised vortices in these systems. Experimental studies of rapidly rotating atomic Bose gases have shown evidence for the formation of ordered arrays of very large numbers of quantised vortices,[1–3] and detailed studies of the structure and dynamics of these vortex lattices have been performed. These studies are consistent with the expected properties for a Bose gas interacting with short range contact interactions (representing the van der Waals’ forces), for which the rotating groundstate is a triangular vortex lattice.

The achievement of Bose-Einstein condensation of chromium-52[4] opens up the possibility of experimental studies of condensates with long-range interactions. Chromium has a large permanent magnetic dipole moment, which leads to significant dipolar interactions in addition to the usual short-range interactions. It is of interest to ask how these long-range interactions affect the vortex lattice groundstates of the rotating condensate. It has been shown[5] that the non-local interactions arising from dipolar interactions can lead to changes in the structure of the vortex lattices. The triangular vortex lattice can be replaced by vortex lattices of different symmetries: square lattice, “stripe crystal” and “bub-

ble crystal” phases. (For a related study of square and stripe crystals see Ref.6.) The vortex lattice structure is therefore a sensitive indication of the form of the interparticle interaction. However, the results of Ref. 5 are restricted to the limit of weak interactions, when the mean interaction energy is smaller than the level spacing of the harmonic trap and the single particle states are restricted to the lowest Landau level (LLL)[7, 8].

In this paper we extend the results of Ref. 5 beyond the weak interaction regime, and determine the vortex lattice structures to be found for arbitrarily strong interactions. For sufficiently weak interactions we recover the results of Ref. 5; we find groundstates that are the square lattice, “stripe crystal” and “bubble crystal” phases predicted in Ref. 5 in the LLL. We determine the effects of Landau level mixing on these states. We show that for strong interactions, these new vortex lattice states are unstable to collapse of the condensate. Our results establish the conditions required in order to observe transitions in the vortex lattice groundstate driven by dipolar interactions.

We also describe the connections with possible “supersolid” states of the *non*-rotating gas, and discuss the stability of these states.

II. FORMULATION

We consider a BEC of atoms with mass M which are confined in a harmonic trap with cylindrical symmetry about the z axis. We denote the trap frequencies by ω_{\parallel} and ω_{\perp} in the axial and transverse directions, and the associated trap lengths by $a_{\parallel\perp} \equiv \sqrt{\hbar/(M\omega_{\parallel\perp})}$. The atoms are taken to interact through both contact interactions and dipolar interactions, with a potential

$$V(\mathbf{r}) = g\delta^3(\mathbf{r}) + C_d V_d(\mathbf{r}), \quad (1)$$

where g parameterizes the contact interactions, and C_d the strength of the dipole interaction potential, $V_d(\mathbf{r})$. We consider the atomic dipole moments to be aligned

with the z axis, as in the recent experiments [4], which sets the functional form for $V_d(\mathbf{r})$. Since the classical dipole-dipole interaction can include also a delta-function contribution[9], for clarity we define the dipolar interaction potential by

$$V_d(\mathbf{r} \neq 0) \equiv \frac{x^2 + y^2 - 2z^2}{(x^2 + y^2 + z^2)^{5/2}} \quad (2)$$

in which we *exclude* the point $\mathbf{r} = 0$, such that any contact contribution of the dipole interaction is contained in the term proportional to g in Eq. (1). We consider the ratio g/C_d to be a parameter that can be varied. For example in the chromium condensate g can be varied experimentally by using a Feshbach resonance [4, 10]. The system can remain stable even for a small attractive contact interaction ($g < 0$). (We note, however, that the $q = 0$ Fourier transform of the effective potential, $\tilde{V}_{q=0}$, should remain positive.)

The results of Ref. 5 suggest that the mean field approximation is excellent even for very dilute systems which may result from fast rotating gases. We thus employ here the Gross-Pitaevskii model. We consider a system, rotating with angular frequency Ω , and containing a large number of vortices, such that near the center of the trap the particle density varies weakly over the scale of the vortex spacing. In the rotating frame, the Hamiltonian becomes equivalent to the Hamiltonian of a particle of charge q in a uniform magnetic field B , with $qB/M = 2\Omega$ [11, 12]. We discretise space and write the kinetic energy for this system in the form [13]

$$E_{\text{kin}} = -t \sum_{\langle i,j \rangle} \Psi_i^* \Psi_j e^{i\phi_{ij}} + \text{c.c.}, \quad (3)$$

where $\langle i,j \rangle$ denotes the nearest neighbours of a square lattice with lattice constant a . In our calculations, the lattice constant a is chosen sufficiently small as to represent the continuum limit, with the particle mass $M = ta^2/\hbar^2$. The ‘‘Peierls’’ phases are defined by the

integral

$$\phi_{ij} = \frac{q}{\hbar} \int_{\mathbf{r}_i}^{\mathbf{r}_j} \mathbf{A} \cdot d\mathbf{l} \quad (4)$$

calculated between the positions of the lattice sites i and j . We choose the Landau gauge for the vector potential $\mathbf{A} = Bx\hat{\mathbf{y}}$, which is convenient in our numerical calculations.

We determine the properties of a large array of vortices by studying the system in a periodic geometry. Imposing periodic boundary conditions under magnetic translations requires that

$$L_x L_y = 2\pi \ell^2 N_v, \quad (5)$$

where N_v is the number of vortices in the simulation cell with dimensions L_x, L_y . The magnetic length $\ell = \sqrt{\hbar/qB} = \sqrt{\hbar/2M\Omega}$ arises as the natural length scale in this system. Since we consider a system containing a large number of vortices, we have $\Omega \simeq \omega_\perp$ [14] so $\ell \simeq a_\perp/\sqrt{2}$. Vortex lattices in periodic systems have been studied previously for the case of contact interactions [15].

Throughout this paper, we work in a quasi-two-dimensional (2D) regime, valid when the confinement in the longitudinal direction is sufficiently strong that the mean interaction energy (which is on the order of the chemical potential μ [16]) is small compared to the level spacing $\hbar\omega_\parallel$. We shall, however, allow mixing of Landau levels for the in-plane motion, so shall work in the regime $\hbar\omega_\parallel \gg \mu \sim \hbar\omega_\perp$ which implies $a_\parallel^2/a_\perp^2 \ll 1$, *i.e.* that the trap is *oblate*. In the quasi-2D limit, $\mu \ll \hbar\omega_\parallel$, the condensate wavefunction is a gaussian along the rotation axis, *i.e.*, $\Psi(x, y, z) = \psi(x, y) e^{-z^2/2a_\parallel^2}/(\pi^{1/4} a_\parallel^{1/2})$. Integrating the dipolar potential energy along the z -axis one obtains the effective dipolar interaction in two dimensions

$$V_d^{2D}(\rho) \equiv \int \int V_d(\rho, z_1 - z_2) \frac{e^{-(z_1^2 + z_2^2)/a_\parallel^2}}{\pi a_\parallel^2} dz_1 dz_2 = \frac{1}{2\sqrt{2\pi} a_\parallel^3} e^{\zeta^2/4} [(2 + \zeta^2) K_0(\zeta^2/4) - \zeta^2 K_1(\zeta^2/4)], \quad (6)$$

where $\rho \equiv \sqrt{x^2 + y^2}$, $\zeta \equiv \rho/a_\parallel$, and K_n are modified Bessel functions. When ρ is large compared to a_\parallel , the expression (6) tends to $1/\rho^3$, which is the dipolar energy for a 2D monolayer. We calculate $1/\rho^3$ by ‘‘Ewald summation’’ for the present case of a *periodic* configuration of dipoles [17], and the remainder $V_d^{2D}(\rho) - 1/\rho^3$ by direct summation within an area with radius several times the length a_\parallel (this combination is rapidly decaying with ρ so it converges quickly).

For the energy minimization we use a variant of a norm-preserving relaxation algorithm which capitalizes on a virial relation [18] in order to fix the wavefunction norm. This is fed with an initial guess and is iterated until an energy minimum is reached. In order to investigate the vortex lattice groundstates, we initially simulate relatively large systems containing $N_v = 8$ or 16 vortices. (Typical numerical grid sizes are $N_x, N_y \sim 50 - 60$.) From these calculations, we find the range of values of

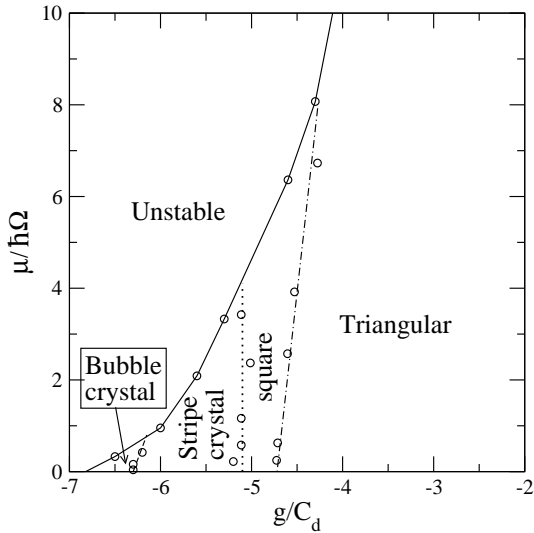


FIG. 1: The phase diagram for a trap asymmetry $a_{\parallel}/\ell = 0.4$. The horizontal axis gives the ratio of the contact to dipolar interactions and the vertical axis is the chemical potential (normalized to the energy corresponding to the rotation frequency Ω of the condensate). The condensate is unstable to collapse on the left of the solid line. Marked on the figure are the regions where vortex lattices of different symmetries are the ground state of the system. The lines are fits to numerical results marked by circles.

the parameters over which the system is stable against collapse. We further identify the symmetries of the vortex lattice groundstates that appear, starting from different initial conditions to give unbiased searches of vortex lattices of different symmetry-types. We subsequently proceed to a systematic calculation of the energy for each of the above mentioned vortex lattice phases by using an appropriate simulation cell that is commensurate with the translational symmetry of that phase. We use a square cell in order to obtain a square vortex lattice (e.g., $N_x = 10, N_y = 10, N_v = 1$), a cell with $N_x/N_y = \sqrt{3}$ for a triangular vortex lattice (e.g., $N_x = 11, N_y = 19, N_v = 2$), and accordingly for the other vortex lattice phases. The typical lattice spacing, implied by Eq. (5), is $\Delta x = \Delta y = 0.25\ell$. We find the energy of each type of vortex lattice as a function of the parameter g/C_d , for various interaction strength values measured by the chemical potential μ . [19]

III. VORTEX LATTICES

The quantitative results depend on the asymmetry of the trap, $a_{\parallel}/a_{\perp} = a_{\parallel}/(\sqrt{2}\ell)$. The phase diagram for the system $a_{\parallel}/\ell = 0.4$ is shown in Fig. 1, as a function of g/C_d and of $\mu/\hbar\Omega$. The limit $\mu \ll \hbar\Omega$ corresponds to the LLL. The region of stability of the system is shown by the solid line. Within the region of stability, we find a series of vortex lattice groundstates which in-

clude the vortex lattices of the symmetries found in the LLL calculation[5]: triangular and square vortex lattices, stripe crystal and bubble crystal phases. (We refer the reader to Ref. 5 for illustrations of the particle distributions in these phases.) The triangular vortex lattice is the lowest energy state for all values of g/C_d to the right of the dashed-dotted line. This includes, in particular, all positive values of g . On the left of the dashed-dotted line a square vortex lattice has energy lower than the triangular one. As g/C_d is further decreased the ground states are stripe crystal phases (in the region between the dotted and the dashed line) which can also be viewed as rectangular lattices of the vortices[5]. We solve for the ground states in this regime by varying the aspect ratio of the simulation cell and optimising the period of the stripes. As g/C_d is decreased the aspect ratio of the rectangular lattice varies, causing the separation between the stripes to become of larger period. For values of g/C_d to the left of the dashed line we find that a bubble crystal phase has the lowest energy. This is a triangular lattice of bubbles (clusters of particles), with the vortices arranged between the bubbles. The simplest bubble crystal phase has four double vortices per bubble which are arranged on the sites of the honeycomb lattice that is dual to the triangular lattice of bubbles[5].

Our results, presented in Fig. 1, show that the values of g/C_d at which there are transitions between the vortex lattice phases are only weakly dependent on the chemical potential, μ . Thus the transitions are closely given by the LLL theory; consistent with this the particle densities we find (not shown) closely resemble those in the LLL[5]. We find that the main effect of going beyond this weak-interaction regime, is the appearance of the instability to collapse for large values of the chemical potential. The value of $\mu/\hbar\Omega$ at which this instability sets in is a strong function of g/C_d . We associate this strong dependence to the varying particle density in these phases. The bubble crystal phase has a very inhomogeneous density, so, for a given average density, the maximum particle density is much larger in the bubble crystal phase than in the triangular vortex lattice. Indeed, in the LLL limit, $\mu \ll \hbar\Omega$, the particle density at the center of the bubble diverges at the point of instability, which is $g/C_d \rightarrow -8.49$ for LLL calculation[5] applied to $a_{\perp}/\ell = 0.4$. [20]

Our results show that for large values of the chemical potential only the triangular vortex lattice is stable. In this limit, $\mu \gg \hbar\Omega$, the vortex cores are small compared to the vortex spacing, and the interactions between the vortices arise from the kinetic energy of the flow around the vortices. This leads to a logarithmic repulsion between the vortices,[21] and thus a triangular lattice groundstate.

An estimate for the region of stability of the triangular vortex lattice in the strongly interacting regime, $\mu/\hbar\Omega \gg 1$, can be obtained by considering the condition for stability of the gas in the regions between the vortices. Denoting the spacing of the triangular vortex lattice by $a_v = [(4\pi)^{1/2}/3^{1/4}]\ell$, we look for an instability to modes

with wavevectors larger than $q = \alpha(2\pi/a_v)$ of a homogeneous Bose gas moving with local velocity $\beta\hbar/(Ma_v)$ (α and β are numerical factors of order one). An analysis of the Bogoliubov spectrum (discussed in more detail below) shows that an instability occurs for

$$\frac{\mu}{\hbar\Omega} > \frac{A}{B \frac{a_{\parallel}}{\ell} \frac{C_d}{g+4\pi C_d} - 1}, \quad (7)$$

where $A = \sqrt{3}/(2\pi)[(2\pi)^2\alpha^2 - 2\beta^2]$ and $B = (2\pi)^2 3^{1/4} \alpha/\sqrt{2}$. The functional form (7) provides a good description of the boundary of stability of the triangular lattice in Fig. 1 at large $\mu/\hbar\Omega$ for reasonable choices of α and β . This theory shows that, for large $\mu/\hbar\Omega \gg 1$, the boundary of stability of the triangular lattice tends to a fixed value $g/C_d = -4\pi + B \frac{a_{\parallel}}{\ell}$ that increases with a_{\parallel}/ℓ . (To determine the precise value of this boundary would require a full solution of the Bogoliubov modes for the triangular vortex lattice in this regime.)

We have investigated the effect of the trap asymmetry by repeating our numerical calculations for $a_{\parallel}/\ell = 0.8$ (a more symmetrical trap). The results for the region of stability, and the phase boundary between triangular and square vortex lattices are qualitatively similar to the case of Fig. 1. We find now that the transitions between the triangular and the square vortex lattices occur for larger values of $g/C_d \simeq -2.6$ as compared to the case $a_{\parallel}/\ell = 0.4$. This is consistent with results in the LLL, and with the qualitative behaviour of (7). Furthermore, the new vortex lattices are stable up to larger values of $\mu/\hbar\Omega$ (up to $\mu/\hbar\Omega \simeq 12$ for the square lattice) for this more symmetrical (less oblate) trap.

In order to observe transitions in the vortex lattice groundstates induced by dipolar interactions, it is necessary both to tune g/C_d to a sufficiently negative value, using for example a Feshbach resonance, and also to ensure that the particle density is sufficiently dilute (or interactions sufficiently weak) that $\mu/\hbar\Omega$ is sufficiently small for the new vortex lattice states to be stable. We see in Fig. 1 that this requires $\mu/\hbar\Omega \lesssim 8$ and $g/C_d \lesssim -4.5$ for the square lattice to be observed. (Stability of the stripe crystal and bubble crystal requires more stringent conditions.) Our numerical calculation gives directly the number of atoms per vortex that correspond to the above conditions. For the parameters relevant for ^{52}Cr [4], and choosing $\Omega = 2\pi \times 100\text{Hz}$, the above conditions require that the number of particles per vortex be $\nu \equiv n_{2d}/n_v \lesssim 1300$. Similarly, for $a_{\parallel}/\ell = 0.8$, the conditions for stability of the square vortex lattice ($\mu/\hbar\Omega \lesssim 12, g/C_d \lesssim -2.5$) lead to $\nu \lesssim 3000$. While it is challenging to achieve a vortex lattice in a sufficiently dilute atomic gas, we note that these conditions are in well excess of what has been achieved in rapidly rotating Rubidium condensates.[1, 3]

Previous calculations of the effects of dipolar interactions on vortex lattices performed in a *trap* geometry[22] found direct transitions from triangular vortex lattice to collapse. It is not straightforward to make direct connections between the present results for the phase diagram

of a *homogeneous* vortex lattice, with those studies on *inhomogeneous* trapped systems. However, we note that in the studies of Ref. 22 the number of vortices is relatively small, so the confinement induces a sizeable variation in the particle density even on the scale of a vortex spacing. It is possible that, owing to the higher particle density at the centre of the trap, a trapped system with a small number of vortices is less stable to collapse. Our results, Fig. 1, apply to a system with a large number of vortices such that density variation over the scale of the vortex lattice constant is small.

IV. NON-ROTATING DIPOLAR BOSE-GAS

We now turn to investigate the non-rotating gas. It is natural to ask whether the stripe and bubble states that appear for a rotating condensate are manifestations of a ‘‘supersolid’’, in which density-wave order appears spontaneously, in the non-rotating groundstate. In the latter case one would expect its response to rotation to involve the vortices being placed in regions of low particle density. Depending on the symmetry of the supersolid state this could lead to particle distributions similar to those of the stripe crystal and bubble crystal states.

A further motivation in this direction if offered by the development of a roton minimum in the excitation spectrum of a homogeneous condensate with dipolar interactions [23, 24] which can touch zero energy at a finite wavevector. This indicates an instability of the homogeneous Bose gas and is suggestive of a possible phase transition to a density-wave state (*e.g.* a condensate of Bogoliubov modes with non-zero wavevector).

The Bogoliubov modes of a quasi-2D homogeneous condensate with dipolar interactions were discussed in Ref. 25. For a gas with density n_{2d} the chemical potential is $\mu = n_{2d}\tilde{V}_{q=0}$, and the excitation spectrum is

$$E(q) = \sqrt{\epsilon_q \left(\epsilon_q + n_{2d}\tilde{V}_q \right)}, \quad \text{where } \epsilon_q = \hbar^2 q^2 / (2M), \quad \text{and} \\ \tilde{V}_q = \frac{g + 4\pi C_d}{\sqrt{2\pi}a_{\parallel}} - 2\pi C_d q e^{q^2 a_{\parallel}^2 / 2} \text{erfc}(qa_{\parallel}/\sqrt{2}) \quad (8)$$

is the Fourier transform of the effective 2D interaction [26].

If, as above, one considers g to be tuned to negative values, the Bogoliubov mode develops a roton minimum that becomes unstable even for the quasi-2D regime, $\mu \ll \hbar\omega_{\parallel}$, for $g/C_d = -4\pi + \sqrt{2\pi^3} C_d n_{2d} / (a_{\parallel} \hbar\omega_{\parallel})$. (The case $g < 0$ was not considered in Ref. 25, and consequently the instability discussed there, for $g \geq 0$, occurs outside of the regime of validity of the quasi-2D approximation, in the crossover to the 3D regime $\mu \simeq \hbar\omega_{\parallel}$.)

We have looked numerically for supersolid states in the quasi-2D Bose gas. We set $\Omega = 0$ in the code used for the numerical calculations described above, chose parameters close to the instability, and looked for stable (or metastable) states of the system. For all parameter values that we have tested (which are in the quasi-2D

regime), we find that the only stable state is the homogeneous Bose gas. Configurations with “supersolid” density wave order (showing a triangular lattice of peaks in the density) are unstable in all cases that we have studied. The collapse mechanism involves a process in which all particles accumulate into one of the peaks, generating a region of the sample in which the density diverges. We have tested this conclusion by independent numerical calculations (based on a discretisation in momentum space, and minimisation by the conjugate gradient method) and have found consistent results. Thus we conclude that, within mean-field theory, there are no stable supersolid phases for an infinite quasi-2D Bose gas with interaction (1).

V. CONCLUSIONS

We have determined the phase diagram for a rapidly rotating atomic Bose gas with dipolar interactions, beyond the weak interaction regime. Our results establish that dipole interactions can drive transitions from the triangular vortex lattice into vortex lattices of various different symmetries. These provide estimates of the experimental parameters that are required in order to observe vortex lattice groundstates of types other than triangular.

We also investigated the fate of a *non*-rotating quasi-2D dipolar Bose gas at the point at which the homogeneous Bose gas becomes unstable to Bogoliubov modes

with a finite wavelength. Our calculations indicate that, within the mean-field approach used, there do not exist stable supersolid states, but that the homogeneous Bose gas becomes unstable to collapse.

The stripe and bubble phases discussed above for a rotating gas are therefore not manifestations of stable supersolid phases of the non-rotating gas. Rather, one should view the rotation as acting to *stabilise* the density-wave order that the dipolar interactions tend to induce in the dipolar Bose gas. The rotation introduces a length-scale, the magnetic length ℓ , which, in the weakly interacting regime $\mu/\hbar\Omega \ll 1$, sets the minimum wavelength over which the condensate wavefunction can vary. This minimum lengthscale prevents collapse of the system provided interactions are sufficiently weak.

Note added: While preparing this work for publication we learned that G. Shlyapnikov and P. Pedri have reached the same conclusion: that putative supersolid states in the quasi-2D Bose gas with the interaction (1) are unstable.[27]

Acknowledgments

This work was partially supported by EPSRC Grant No. GR/S61263/01 and by the ICAM Senior Fellowship programme (NRC).

-
- [1] V. Bretin, S. Stock, Y. Seurin, and J. Dalibard, Phys. Rev. Lett. **92**, 050403 (2004).
- [2] J. Abo-Shaer, C. Raman, J. Vogels, and W. Ketterle, Science **292**, 476 (2001).
- [3] V. Schweikhard, I. Coddington, P. Engels, V.P. Mogenдорff, E.A. Cornell, Phys. Rev. Lett. **92**, 040404 (2004).
- [4] A. Griesmaier, J. Werner, S. Hensler, J. Stuhler, T. Pfau, Phys. Rev. Lett. **94**, 160401 (2005).
- [5] N.R. Cooper, E.H. Rezayi, and S.H. Simon, Phys. Rev. Lett. **95**, 200402 (2005).
- [6] J. Zhang and H. Zhai, Phys. Rev. Lett. **95**, 200403 (2005).
- [7] D. Butts and D. Rokhsar, Nature (London) **397**, 327 (1999).
- [8] N.K. Wilkin, J.M.F. Gunn, and R.A. Smith, Phys. Rev. Lett. **80**, 2265 (1998).
- [9] J. D. Jackson, *Classical Electrodynamics*, 3rd ed. (Wiley, New York, 1999).
- [10] J. Werner *et al.*, Phys. Rev. Lett. **94**, 183201 (2005).
- [11] N.R. Cooper, N.K. Wilkin, and J.M.F. Gunn, Phys. Rev. Lett. **87**, 120405 (2001).
- [12] T.-L. Ho, Phys. Rev. Lett. **87**, 060403 (2001).
- [13] N. Nagaosa, *Quantum Field Theory in Condensed Matter Physics* (Springer, Berlin, 1998).
- [14] Using a Thomas-Fermi approximation for a harmonically trapped gas with a large number of vortices, it is simple to show that $\frac{\omega_{\perp}^2}{\Omega^2} = 1 + \frac{2\mu}{\hbar\Omega} \frac{1}{N_v}$. Thus $\omega_{\perp}/\Omega \rightarrow 1$ at $N_v \rightarrow \infty$. Thus $\omega_{\perp}/\Omega \rightarrow 1$ at $N_v \rightarrow \infty$.
- [15] M. Cozzini, S. Stringari, and C. Tozzo, Phys. Rev. A **73**, 023615 (2006).
- [16] We define the chemical potential to be measured relative to the zero-point energy in the rotating frame, $\hbar\Omega + (1/2)\hbar\omega_{\parallel}$.
- [17] J.-J. Weiss, J. Phys.: Condens. Matter **15**, S1471 (2003).
- [18] N. Papanicolaou, S. Komineas, and N.R. Cooper, Phys. Rev. A **72**, 053609 (2005).
- [19] Since the different vortex phases have different unit cells they cannot all be simulated with the same value of the lattice discretisation Δx . In order to minimize the effects of discretisation, we compute each for a range of lattices with a range of Δx , and interpolate these results so that the energy comparison is made at the same value of Δx .
- [20] In Fig.1 as $\mu \rightarrow 0$ we find that the system is stable for $g/C_d > -6.8$. The discrepancy from the LLL result, $g/C_d = -8.49$ is due to our discretization of the condensate wavefunction in the present work (for finer grids we find improved agreement with the LLL result), so can be viewed as a measure of the numerical errors of the present calculation.
- [21] R. Donnelly, *Quantized vortices in Helium II* (Cambridge University Press, Cambridge, 1991).
- [22] S. Yi and H. Pu, Phys. Rev. A **73**, 061602(R) (2006).

- [23] D.H.J. O'Dell, S. Giovanazzi, and C. Eberlein, Phys. Rev. Lett. **92**, 250401 (2004).
- [24] L. Santos, G. V. Shlyapnikov, and M. Lewenstein, Phys. Rev. Lett. **90**, 250403 (2003).
- [25] U.R. Fischer, Phys. Rev. A **73**, 031602(R) (2006).
- [26] Note that by excluding the point $r = 0$ our definition of the dipolar interaction (2) differs from that of Ref. 25 by a contact term (a constant in momentum space).
- [27] G. Shlyapnikov and P. Pedri, conference on "Correlated and Many-Body Phenomena in Dipolar Systems", June 2006, Dresden.